

# Observing dynamic oscillatory behavior of triple points among black hole thermodynamic phase transitions

Shao-Wen Wei<sup>1,2 \*</sup>, Yong-Qiang Wang<sup>1,2 †</sup>, Yu-Xiao Liu<sup>1,2 ‡</sup>, and Robert B. Mann<sup>3 §</sup>

<sup>1</sup>Lanzhou Center for Theoretical Physics, Key Laboratory of Theoretical Physics of Gansu Province, School of Physical Science and Technology, Lanzhou University, Lanzhou 730000, People's Republic of China

<sup>2</sup>Institute of Theoretical Physics & Research Center of Gravitation, Lanzhou University, Lanzhou 730000, People's Republic of China

<sup>3</sup>Department of Physics and Astronomy, University of Waterloo, Waterloo, Ontario, Canada, N2L 3G1  
(Dated: February 2, 2021)

Understanding the dynamic process of black hole thermodynamic phase transitions at a triple point is a huge challenge. In this letter, we carry out the first investigation of dynamical phase behaviour at a black hole triple point. By numerically solving the Smoluchowski equation near the triple point for a six-dimensional charged Gauss-Bonnet anti-de Sitter black hole, we find that initial small, intermediate, or large black holes can transit to the other two coexistent phases at the triple point, indicating that thermodynamic phase transitions can indeed occur dynamically. More significantly, we observe characteristic weak and strong oscillatory behaviour in this dynamic process, which can be understood from an investigation of the rate of first passage from one phase to another. Our results further an understanding of the dynamic process of black hole thermodynamic phase transitions.

PACS numbers: 04.70.Dy, 68.35.Rh, 04.50.Kd, 02.50.-r.

*Introduction* Black holes are now widely believed to behave as thermodynamic systems after the establishment of the four laws of black hole thermodynamics [1–3]. As such, they can be expected to undergo phase transitions, one of the first being the well-known Hawking-Page phase transition [4]. Over the past decade it has been shown that black holes exhibit an abundance of phase behaviour [5], upon interpreting the cosmological constant in anti-de Sitter (AdS) space as the pressure of the black hole system in extended phase space [6, 7]. Known as black hole chemistry, small/large charged black hole phase transitions take place, reminiscent of the liquid-gas phase transition of a Van der Waals (VdW) fluid [6, 7].

Recently studies of the dynamics of phase transitions have been carried out [8–10] by solving a special case of the Fokker-Planck equation known as the Smoluchowski equation (SE). A dynamic transition indeed occurs between the unstable and stable black hole phases, and further investigation confirmed that even between stable small and large black hole phases, the dynamic process can also occur [11]. The SE has been also been used to study analytically the evolution of the black hole mass distribution and supermassive black hole merger rates [12, 13].

The discovery of black hole triple points [14–16] strengthens the chemical interpretation of black hole thermodynamics. It suggests that some black hole systems are similar to water, where solid, liquid, and gas phases can coexist, with the triple point being a coexis-

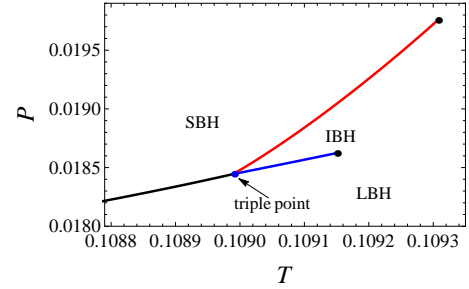


FIG. 1: Phase structures near the triple point for the six dimensional charged GB-AdS black holes with  $Q=0.2$  and  $\alpha=1.06$  in the  $P$ - $T$  diagram. “SBH”, “IBH”, and “LBH” are for the small, intermediate, and large black holes.

tence phase of stable small, intermediate, and large black holes. Across the triple point, the three phases can transition into one another. Consequently triple points expose significant characteristic properties of the system. However the dynamics of this transition process for black holes is still unknown.

In this paper, we aim to test and uncover such dynamic processes. In so doing we shall discover important properties for further understanding black hole thermodynamics and, by implication, their underlying degrees of freedom.

*Triple point in black hole systems* In order to exhibit the rich structure of the triple point, we start with the six-dimensional charged Gauss-Bonnet (GB) AdS black holes [15, 16]. The corresponding equation of state in the extended phase space reads

$$P = \frac{T}{r_h} - \frac{3}{4\pi r_h^2} + \frac{2\alpha T}{r_h^3} - \frac{\alpha}{4\pi r_h^4} + \frac{Q^2}{8\pi r_h^8}, \quad (1)$$

\*E-mail: weishw@lzu.edu.cn

†E-mail: yqwang@lzu.edu.cn

‡E-mail: liuyx@lzu.edu.cn

§E-mail: rbmann@uwaterloo.ca

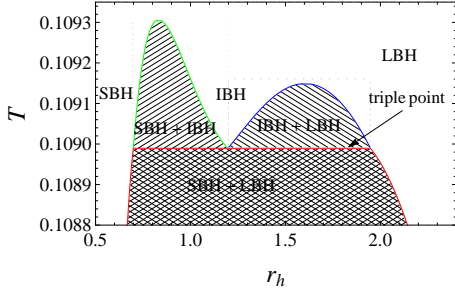


FIG. 2: Phase structures near the triple point in the  $T$ - $r_h$  space, with  $Q = 0.2$  and  $\alpha = 1.06$ .

where  $P$  and  $T$  is the pressure and temperature of the black hole system. All quantities are measured in Planck units, with  $\alpha$  the GB coupling parameter,  $Q$  denoting the black hole charge, and  $r_h$  the horizon radius, characterizing the size of the black hole as either small, intermediate, or large [5, 17–20].

This equation of state possesses a triple point, shown as a blue dot in Fig. 1 in the  $P$ - $T$  phase diagram, where  $Q=0.2$  and  $\alpha=1.06$ . The other two black dots signify critical points, where the phase transition is second order. The diagram is quite similar to that of the phase structure of water, except that coexistence curve of small and intermediate black holes has a positive slope. The degenerate coexistence regions in the  $P$ - $T$  diagram are better illustrated in a  $T$ - $r_h$  phase diagram, shown in Fig. 2 for the first time. The two critical points are located at the two peaks, and the triple point becomes a horizontal line, along which these three black hole coexistence phases can coexist. Correspondingly, these phases have the same free energy, with the Gibbs free energy exhibiting double swallow tail behaviour with both swallowtail intersections coinciding [15, 16]. It is possible to construct two pair equal area regions on each isothermal curve, but we will not pursue this as we are interested in the dynamic process of the phase transition.

Consider a canonical ensemble at temperature  $T_E$  (and not the Hawking temperature), composed of a series of black hole spacetimes (called the landscape) with arbitrary horizon radius, and define a new Gibbs free energy

$$G_L = H - T_E S \quad (2)$$

$$= \frac{2\pi r_h^5}{15} \left( 4\pi P - \frac{5\pi T_E}{r_h} + \frac{5}{r_h^2} - \frac{20\pi\alpha T_E}{r_h^3} + \frac{5\alpha}{r_h^4} \right) + \frac{\pi Q^2}{9r_h^3}$$

where  $H$  and  $S$  are the respective enthalpy and entropy on the landscape [8]. This generalized off-shell free energy describes transient black hole states, with  $r_h$  the order parameter, describing the underlying microscopic degrees of freedom [9].

We illustrate  $G_L$  at the triple point in Fig. 3 for an ensemble temperature  $T_E=0.108$  with  $Q=0.2$ ,  $P=0.018164$ ,  $\alpha=1.080978$ ,  $r_{hs}=0.667162$ ,  $r_{hi}=1.313823$ ,  $r_{hl}=1.884450$ ,  $r_{m1}=0.905109$ , and  $r_{m2}=1.626470$ . Each point on this curve denotes a black hole state. However, not all of

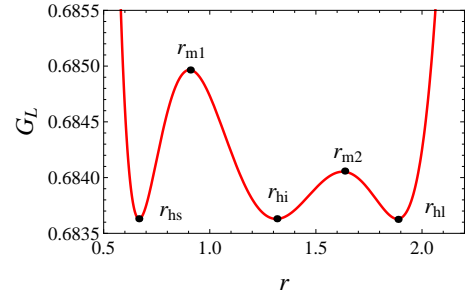


FIG. 3: Behavior of the Gibbs free energy via landscape at the triple point with  $Q=0.2$ ,  $T_E=0.108$ , and  $P=0.018164$ .

them are actual black hole solutions of the Einstein GB equations. Only the local extrema correspond to actual black holes, while the others are off-shell transient states [11]. The local minima and maxima denote thermodynamic stable or unstable black holes. Combining the fact that a stable thermodynamic system has the lowest free energy, the black hole system will migrate to (or remain at) the well of the deepest depth. For the parameter choice employed in Fig. 3, the three wells have the same depth, indicating a triple point where the black hole system can be in any arbitrary combination of these three states. More interestingly, the two peaks have different heights, which govern the transit rate between the various black hole states [9]. Slightly changing the pressure or temperature, we can obtain another triple point, with the general structure of Fig. 3 holding, with the height of the peaks changing accordingly.

*Dynamic processes at the triple point* Based on the behavior of the Gibbs free energy  $G_L$ , we examine the dynamic properties of black hole phase transitions at the triple point. Given an initial state in the black hole system (e.g. a small black hole), at the triple point it will evolve via a diffusion process to other states since it can undergo thermodynamic phase transitions. We denote  $\rho(r_h, t)$  as the probability distribution of the system staying at a given black hole state. The SE [21]

$$\frac{\partial \rho(r, t)}{\partial t} = D \frac{\partial}{\partial r} \left( e^{-\frac{\beta G_L(r)}{k_B T_E}} \frac{\partial}{\partial r} \left( e^{\frac{\beta G_L(r)}{k_B T_E}} \rho(r, t) \right) \right) \quad (3)$$

governs this behaviour, where we have replaced  $r_h$  with  $r$  for simplicity. The diffusion coefficient  $D = k_B T_E / \zeta$  with  $k_B$  and  $\zeta$  being the Boltzman constant and dissipation coefficient. Without loss of generality, we set  $k_B = \zeta = 1$  in the following, and choose the initial state to be a Gaussian wave packet

$$\rho(r, 0) = \frac{1}{0.005\sqrt{\pi}} e^{-\frac{(r-r_j)^2}{0.005^2}} \quad (4)$$

located at  $r_j$ . Setting  $r_j = r_{hs}$ ,  $r_{hi}$ , or  $r_{hl}$  respectively means the initial state is peaked at a coexistent small, intermediate, or large black hole state. By imposing reflective boundary conditions at  $r = 0$  and  $r = \infty$  (sufficiently large distance), we numerically solve the SE equation for

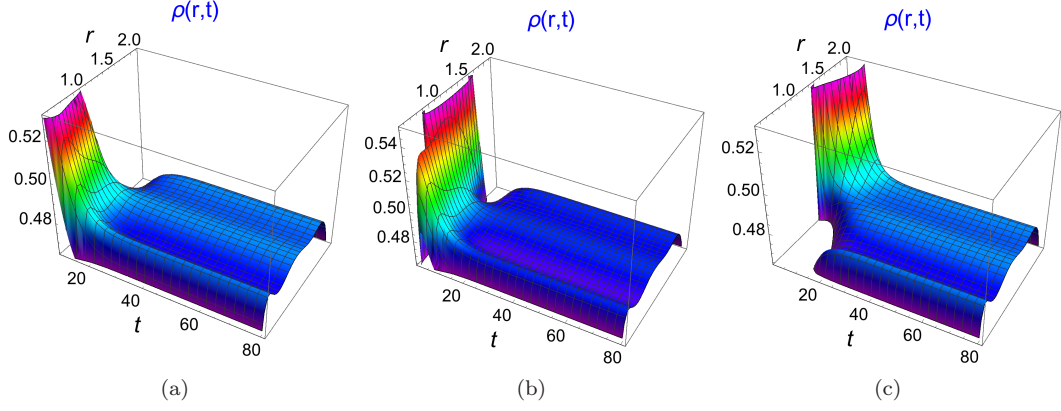


FIG. 4: Probability distribution  $\rho(r,t)$  governed by the SE equation with  $Q=0.2$ ,  $T_E=0.108$ , and  $P=0.018164$ . The initial Gaussian wave packet, respectively, located at (a) small black hole state, (b) intermediate black hole state, and (c) large black hole state.

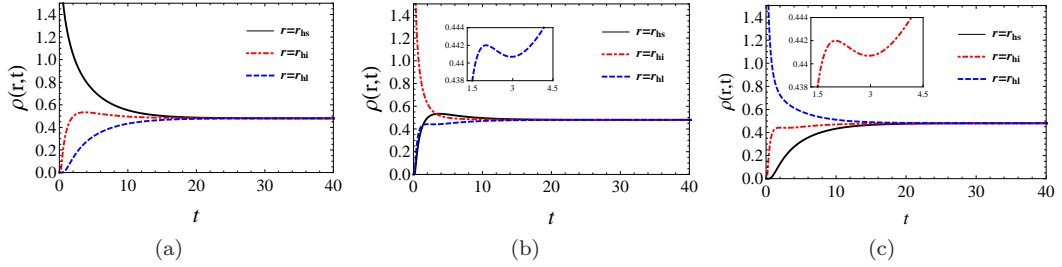


FIG. 5: Behaviors of the probability  $\rho(r,t)$  at the coexistence small, intermediate, and large black hole states, when the initial Gaussian wave packet is peaked at the coexistent (a) small (b) intermediate and (c) large black hole states.

each case, illustrating the results in Fig. 4. Regardless of the choice of initial state, we observe that the probability  $\rho(r,t)$  leaks to other states, implying that there are indeed phase transitions between these three coexistent states. This takes place very quickly: within  $t = 80$  the system attains its final stationary state, with the local maxima of  $\rho(r,t)$  at the location of these three coexistent black holes. More detailed study indicates that these maxima share the same value  $\rho(r_k, t) = 0.4801$ , for  $k = \text{hs, hi, and hl}$ , indicating that the black hole system settles into a combination of these coexistent phases. Moreover, this specific value is independent of the initial state, which can be understood from the SE. After a sufficiently long time the system approaches stationarity;  $\rho(r,t)$  will no longer change, and so the left side of (3) vanishes. The probability distribution is then only determined by  $G_L$  in (2).

This dynamic phase transition process at the triple point is quite different from that of a VdW type phase transition [9–11]. We now examine the detailed evolution of each coexistent black hole phases, plotting in Fig. 5 the behaviour of  $\rho(r_k, t)$  for  $k = \text{hs, hi, and hl}$ , when the initial Gaussian wave packet is respectively peaked at these states. We see that the initially large value  $\rho(r_k, t)$  in

each case rapidly decays to a stationary value, whilst the other two states (initially zero) grow toward this value.

Considering first Fig. 5(a), the initial Gaussian wave packet  $\rho(r, 0)$  is peaked at the small black hole phase with  $\rho(r_{\text{hs}}, 0)$  large, while  $\rho(r_{\text{hi}}, 0)$  and  $\rho(r_{\text{hl}}, 0)$  are negligibly small. As  $t$  increases  $\rho(r_{\text{hs}}, t)$  decreases, and  $\rho(r_{\text{hi}}, t)$  and  $\rho(r_{\text{hl}}, t)$  increase as expected, the latter more slowly since the initial state must surmount two barriers. The transition rate from the small to intermediate black hole state is higher than the total rate from intermediate to small and large black hole states. Once  $t \geq 40$ , all of them tend to 0.4801, where the final stationary state is achieved. During the evolution, we observe an interesting phenomenon for  $\rho(r_{\text{hi}}, t)$ : it increases to a maximum of 0.5338 at  $t = 3.6986$  and then decreases with time to its stationary value of 0.4801. This presumably takes place because the intermediate black hole state can transit to both small and large black hole states, the latter much more easily due to the smaller barrier between the intermediate and large black hole states, shown in Fig. 3. As the large black hole state becomes more populated, it will transit back to the intermediate one, reducing the rate of the latter. Since  $\rho(r_{\text{hi}}, t) < \rho(r_{\text{hs}}, t)$ , we refer to this novel behaviour as a weak oscillatory phenomenon.

Corresponding behaviour is also observed when the initial wave packet is peaked at the intermediate black hole state, shown in Fig. 5(b). Here more fine structure is present. As expected,  $\rho(r_{\text{hi}}, t)$  decreases whereas  $\rho(r_{\text{hs}}, t)$  and  $\rho(r_{\text{hl}}, t)$  both increase, with the former reaching a maximum of 0.5337 at  $t = 3.6987$ . At early times, these probability distributions exhibit interesting behaviour. When  $0 < t < 1.3840$ , we find that the probability leaks from the intermediate to both small and large black hole states, with  $\rho(r_{\text{hl}}, t)$  increasing faster than  $\rho(r_{\text{hs}}, t)$  due to the lower barrier height. This pattern reverses for  $t > 1.3840$ . Once  $t > 3.2995$ ,  $\rho(r_{\text{hs}}, t)$  is dominant among the three probabilities, indicating that the system has a large probability to stay at the coexistent small black hole state. For a short time afterward  $\rho(r_{\text{hs}}, t)$  continues to grow to its maximum, after which it decays to stationarity, transiting back to the coexistent intermediate and large black hole states. Since  $\rho(r_{\text{hs}}, t)$  eventually dominates we refer to this as a strong oscillatory phenomenon. In Fig. 5(c) we see that for all  $t$ ,  $\rho(r_{\text{hl}}, t) > \rho(r_{\text{hi}}, t) > \rho(r_{\text{hs}}, t)$ . However we also observe additional (tiny) oscillatory behaviour (shown in the insets in Fig. 5(b) and 5(c)) when the initial wavepacket is initially peaked at the coexistent intermediate or large black hole phases.

*First passage event* We seek here more clues about this oscillatory phenomena from the distribution of first passage times of the phase transition. This is defined as the rate at which a given initial state first reaches an unstable black hole phase, represented by the peak of the free energy [9]. From Fig. 3 we have three cases: small to intermediate (case I), intermediate to small and large (case II), and large to intermediate (case III). For all cases we impose reflective boundary condition at  $r = 0$  and  $r = \infty$  (sufficiently large  $r$ ) and absorbing boundary conditions at the peaks  $r_{m1}$  and  $r_{m2}$ , accordingly, where the latter model a given coexistent state first leaving the system. Note that such conditions do not preserve normalization of the probability distribution. Using the SE, we can express the first passage rate  $F_P(t)$  for these three cases as

$$F_{P1}(t) = -\frac{\partial \rho(r_{m1}, t)}{\partial r}, \quad (5)$$

$$F_{P2}(t) = \frac{\partial \rho(r_{m1}, t)}{\partial r} - \frac{\partial \rho(r_{m2}, t)}{\partial r}, \quad (6)$$

$$F_{P3}(t) = \frac{\partial \rho(r_{m2}, t)}{\partial r}, \quad (7)$$

where  $F_{P2}(t) \neq -(F_{P1}(t) + F_{P3}(t))$  since each case has different boundary conditions.

The numerical results are given in Fig. 6(a). For each case, there is a single peak, respectively at  $t_1=0.0876$ ,  $t_2=2.3725$ , and  $t_3=0.1026$ , which can be interpreted as the length of time at which the system remains in its initial state for each case before first transiting to another state. For cases I and III the system first transits to other states after a short time, whereas for case II the system remains in the intermediate black hole state somewhat

longer. This expectation is borne out from the mean first passage time

$$\langle t \rangle = \int_0^\infty t F_P dt, \quad (8)$$

for each case, where we find  $\langle t_1 \rangle = 0.86$ ,  $\langle t_2 \rangle = 2.37$ ,  $\langle t_3 \rangle = 1.75$  (where  $0 < t < 40$ ).

For case I, the initial state is at the coexistent small black hole state. As time increases, its probability  $\rho(r_{\text{hs}}, t)$  decreases and leaks to the intermediate black hole state. Since  $\langle t_2 \rangle$  is larger than  $\langle t_1 \rangle$  and  $\langle t_3 \rangle$ , the system will stay longer at the intermediate black hole state. Then it will transit back to the coexistent small or large black hole states. Consequently  $\rho(r_{\text{hi}}, t)$  first increases then decreases with time, and thus weak oscillatory behavior is present in Fig. 5(a).

We find that  $F_P(t)$  is governed not only by the barrier height, as discussed previously [8, 9], but also by the barrier width. An inspection of Fig. 3 indicates that the difference in barrier heights  $\Delta G_L = G_{m1} - G_{m2} \simeq 0.001$ , whereas the difference in barrier widths is  $\Delta r_{m1} - \Delta r_{m2} \simeq 0.02$ , 20 times larger than  $\Delta G_L$ . These larger barrier width values will dominate over the small barrier height difference, with smaller values of  $\Delta r$  leading to a peak in  $F_P(t)$  at small  $t$ . Since  $\Delta r_{m1} = 0.2379$  (case I) is slightly smaller than  $\Delta r_{m2} = 0.2580$  (case III), we have  $t_1 < t_3$ . For case II absorbing boundary conditions are imposed at both sides, and so the intermediate black hole can transit to large and small black holes through the right and left boundaries respectively. Since the right barrier is lower than the left one and closer to the well, the peak of the second part of  $F_{P2}(t)$  corresponds to a small time, exactly the situation shown in Fig. 6(b).

In order to understand the strong oscillatory behavior shown in Fig. 5(b), we, respectively, plot the two parts of  $F_{P2}(t)$  with red solid and blue dashed curves in Fig. 6(b). The first and second parts denote the transitions to the small and large black hole states. Their peaks are at  $t_{i1}=0.2568$  and  $t_{i2}=0.1507$ , and we find that the lower barrier corresponds to a higher peak at shorter time. However, we find from (8) that  $\langle t_{i1} \rangle = 0.28 < \langle t_{i2} \rangle = 0.31$ . Hence  $\rho(r_{\text{hs}}, t)$  will at some time become larger than  $\rho(r_{\text{hl}}, t)$ . Thus strong oscillatory behavior is exhibited when the initial state is peaked at the coexistent intermediate black hole state. The fact that  $t_{i1} > t_{i2}$  indicates that  $\rho(r_{\text{hl}}, t)$  increases faster than  $\rho(r_{\text{hs}}, t)$  at early transition times.

Moreover, apart from the coexistence with the small black hole state, we find that the Gibbs free energy  $G_L$  is approximately symmetric about  $r_{m2}$ . Hence  $\rho(r_{\text{hi}}, t)$  and  $\rho(r_{\text{hl}}, t)$  exhibit similar behavior when the initial wave packet is located at coexisting intermediate or large black hole states. From Figs. 5(b) and 5(c), we observe  $\rho(r_{\text{hi}}, t)$  and  $\rho(r_{\text{hl}}, t)$  share approximately the similar tiny oscillatory behavior with time, as shown in the insets. The presence of these tiny oscillations is due to coexistence with the small black hole state.

*Summary* We have carried out the first investigation



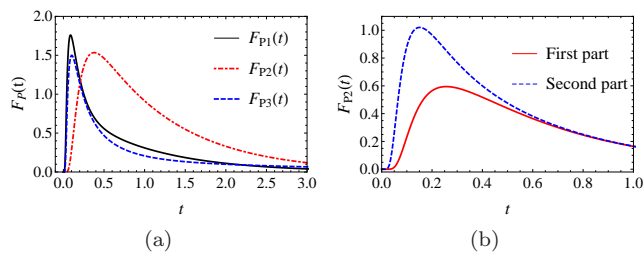


FIG. 6: (a) First passage time rate for case I, II, and III. (b) The first and second parts of the first passage time for  $F_{P2}(t)$ .

of dynamical phase behaviour at a black hole triple point. The degenerate triple point in a  $P$ - $T$  phase diagram becomes a horizontal line in the  $T$ - $r_h$  phase diagram, with each coexistence region explicitly displayed. On the free energy landscape, with  $r_h$  as the order parameter, the characteristic pattern of the triple point is that of three potential wells of the same depth, with the coexistent black hole phases located at the minima of the wells.

Transitions between these different phases are quite different from that of first order VdW type phase transitions, and can be studied dynamically via the Smoluchowski equation. We find that, regardless of the initial

phase in the black hole system, each phase can transit into the others, attaining stationarity of all three phases after a short time. More significantly, we observe both weak oscillatory behaviour, in which the probability distribution of one state attains a maximal value before decaying to stationarity, and strong oscillatory behaviour, in which this maximum dominates over the other two states. A study of the mean first passage time indicates that if the system is initially in the intermediate black hole state, it takes longer to transit to one of the other states than for the other two cases.

Our results indicate that black holes have interesting dynamical phase behaviour whose relationship to their underlying degrees of freedom remains to be understood. It would be interesting to apply our approach to other black hole systems with various types of phase transitions, including angular momenta [22], hair [23–25], and acceleration [26, 27], where more interesting dynamic phenomena should be observed.

*Acknowledgements.*—This work was supported by the National Natural Science Foundation of China (Grants No. 12075103, No. 11675064, No. 11875151, and No. 12047501) and the Natural Sciences and Engineering Research Council of Canada.

- 
- [1] S. W. Hawking, Commun. Math. Phys. **43**, 199 (1975).
  - [2] J. D. Bekenstein, Phys. Rev. D **7**, 2333 (1973).
  - [3] J. M. Bardeen, B. Carter, and S. Hawking, Commun. Math. Phys. **31**, 161 (1973).
  - [4] S. W. Hawking and D. N. Page, Commun. Math. Phys. **87**, 577 (1983).
  - [5] D. Kubiznak, R. B. Mann and M. Teo, Class. Quant. Grav. **34**, no.6, 063001 (2017), [arXiv:1608.06147 [hep-th]].
  - [6] D. Kastor, S. Ray, and J. Traschen, Class. Quant. Grav. **26**, 195011 (2009), [arXiv:0904.2765 [hep-th]].
  - [7] D. Kubiznak and R. B. Mann, J. High Energy Phys. **1207**, 033 (2012), [arXiv:1205.0559 [hep-th]].
  - [8] R. Li, and J. Wang, Phys. Rev. D **102**, 024085 (2020).
  - [9] R. Li, K. Zhang, and J. Wang, J. High Energy Phys. **2010**, 090 (2020), [arXiv:2008.00495 [hep-th]].
  - [10] R. Li and J. Wang, [arXiv:2012.05424 [gr-qc]].
  - [11] S.-W. Wei, Y.-X. Liu, and Y.-Q. Wang, [arXiv:2009.05215 [gr-qc]].
  - [12] H. Mouri and Y. Taniguchi, Astrophys. J. Lett. **566**, L17 (2002), [astro-ph/0201102 [astro-ph]].
  - [13] A. L. Erickcek, M. Kamionkowski, and A. J. Benson, Mon. Not. Roy. Astron. Soc. **371**, 1992 (2006), [astro-ph/0604281 [astro-ph]].
  - [14] N. Altamirano, D. Kubiznak, R. B. Mann, and Z. Sherkatghanad, Class. Quant. Grav. **31**, 042001 (2014), [arXiv:1308.2672 [hep-th]].
  - [15] S.-W. Wei and Y.-X. Liu, Phys. Rev. D **90**, 044057 (2014), [arXiv:1402.2837 [hep-th]].
  - [16] A. M. Frassino, D. Kubiznak, R. B. Mann and F. Simovic, J. High Energy Phys. **09**, 080 (2014), [arXiv:1406.7015 [hep-th]].
  - [17] D. G. Boulware and S. Deser, Phys. Rev. Lett. **55**, 2656 (1985).
  - [18] R. G. Cai, Phys. Rev. D **65**, 084014 (2002), [arXiv:hep-th/0109133].
  - [19] M. Cvetič, S. Nojiri, and S. D. Odintsov, Nucl. Phys. B **628**, 295 (2002), [arXiv:hep-th/0112045].
  - [20] R.-G. Cai, L.-M. Cao, L. Li, and R.-Q. Yang, J. High Energy Phys. **1309**, 005 (2013), [arXiv:1306.6233 [gr-qc]].
  - [21] R. Zwanzig, *Nonequilibrium Statistical Mechanics*, Oxford University Press (2001).
  - [22] N. Altamirano, D. Kubiznak, R. B. Mann and Z. Sherkatghanad, Galaxies **2**, 89 (2014), [arXiv:1401.2586 [hep-th]].
  - [23] G. Giribet, M. Leoni, J. Oliva, and S. Ray, Phys. Rev. D **89**, 085040 (2014), [arXiv:1401.4987 [hep-th]].
  - [24] R. A. Hennigar, E. Tjoa, and R. B. Mann, J. High Energy Phys. **1702**, 070 (2017), [arXiv:1612.06852 [hep-th]].
  - [25] H. Dykaar, R. A. Hennigar and R. B. Mann, J. High Energy Phys. **1705**, 045 (2017), [arXiv:1703.01633 [hep-th]].
  - [26] A. Anabalon, M. Appels, R. Gregory, D. Kubiznak, R. B. Mann, and A. Ovgun, Phys. Rev. D **98**, 104038 (2018), [arXiv:1805.02687 [hep-th]].
  - [27] A. Anabalon, F. Gray, R. Gregory, D. Kubiznak, and R. B. Mann, J. High Energy Phys. **1904**, 096 (2019), [arXiv:1811.04936 [hep-th]].